JOURNAL OF MATERIALS SCIENCE **34** (1999) 283–290

Development of a methodology for assessing the integrity of dental restorations

S. P. D'ARCY, D. G. GORMAN
Department of Engineering, Aberdeen University, Aberdeen, UK
E-mail: susan@astecdev.co.uk

W. P. SAUNDERS
University of Glasgow Dental School, Glasgow, UK

R. M. TAYLOR
School of Mechanical and Offshore Engineering, The Robert Gordon University, Aberdeen, UK

This paper describes an experimental methodology for assessing the combined effect of differing endodontic posts and cements, which are important structural elements of restorations for the root filled tooth. The focus is upon the strength of the restoration when subjected to cyclic combined direct and torsional shear forces at magnitudes and frequencies representative of those present during normal mastication. The paper describes the experimental facilities and procedures with respect to the modelling of the restoration and application of the loads. After a predetermined number of load cycles the modelled restoration is removed and examined in detail using microleakage techniques.

1. Introduction

The long term structural integrity of a restoration in a root filled tooth is influenced by a combination of clinical factors and the selection of the critical components which constitute the restoration. With respect to the latter, the two components which have the major influence upon structural integrity are the design of the endodontic post and choice of cement. Research into endodontic posts has been predominantly concentrated around comparing the properties of various commercially available posts. For example, references [1, 2 and 3] describe research in which commercial designs of endodontic post were investigated to determine which provides the highest level of retention when subjected to tensile force. For each design of post, the tensile force was applied by means of a simple "pull-out" test on the post, which had been inserted and cemented into a pre-prepared channel in the root of a natural tooth. Pull-out tests have also been used in the assessment of dental cements [4, 5]. This type of test has been used for some time, and the results from it have been hitherto accepted by clinicians as a benchmark by which endodontic posts can be compared. However, the significance of this test is not clear [6] since it does not comprehensively represent the types of forces which the post would actually experience *in-vivo*. There are other components of force to which a restoration is subjected, and these must be taken into consideration when assessing their performance. Torsional forces are applied to teeth as a matter of course because of masticatory patterns. When occlusal forces are applied to post-crowns, twisting and bending moments may be induced. If the occlusal contacts in the inter-cuspal position occur eccentrically, then a moment will be produced and the torsional forces applied to the crown will be transmitted to the post. This causes shear forces between the post and cement and also between the cement and dentine. In practice, a clinician will often include some form of antirotational device in this type of restoration. Although dental restorations are subjected to these forces, from the literature there would appear to be no previous investigations carried out into the direct and dedicated effects of these forces, despite the frequency of their occurrence [7].

This paper therefore describes a programme of research the aim of which was to develop a methodology for assessing the combined behavior of endodontic post and cements whilst subjected to cyclic, combined direct and torsional shear forces. Post load analysis is conducted using microleakage studies, which have been used in dental research to establish the extent of cracking experienced by a restoration as a result of thermal cycling [8] and fatigue loading [9, 10].

2. Method

Test pieces representing the tooth and crown system were constructed in the following manner. An endodontic post was inserted into a prepared channel in a block of beechwood (Fig. 1). Beechwood has been used previously in orthopaedic investigations because its properties are similar to those of human cancellous bone [11, 12]. Further investigation revealed that the properties of beechwood were closer to human dentine than

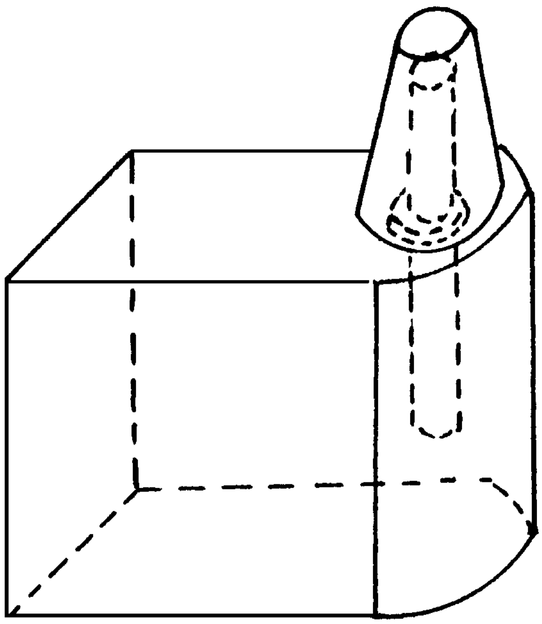

Figure 1 Beechwood "tooth" component of test piece.

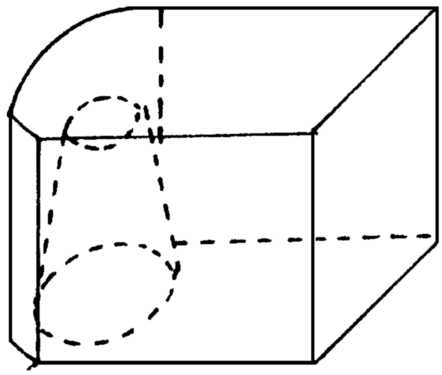

Figure 2 Perspex "crown" component of test piece.

human bone, and thus it was selected for use in this study [13]. The post was cemented in position following the instructions supplied with the posts (Essential Dental Systems, 1993) by an experienced clinician and was cemented in place using proprietary 3M Vitremer luting cement (3M Dental Products, St. Paul MN, USA).

A core was then built up on the crown in a manner similar to that used in practice when constructing a restoration, using a standard size mould to ensure repeatability of the core dimensions. These cores were built up using 3M Vitremer cement. A perspex piece (Fig. 2) was used to represent the crown. In order to establish that the system provided a tool for identifying the effect of varying different aspects of the system, one component of the system was changed, in this instance the type of cement. The crown was cemented onto the core of the system using one of three commonly used dental cements: Resin Modified Glass Ionomer (RMGI) (3M Vitremer luting cement^{TM}, 3M Dental Products, St. Paul MN, USA), Composite Resin Cement (CRC) (3M Scotchbond^{TM}, 3M Dental Products, St. Paul, MN, USA) or Zinc Phosphate ($ZnPO_4$) (De Trey Zinc, Dentsply Limited, Weybridge, Surrey, UK). The same type of post was used throughout the testing, namely, Flexi-flange (Essential Dental Systems, Inc., S. Hackensack, New Jersey, USA). Cementation of the crown was carried out following manufacturers' instructions and once constructed, test pieces were maintained at a temperature of 37 °C (body temperature) in an environment of 100% humidity, thus representative of the oral environment. In order to prevent swelling of the beechwood, each test piece was coated in 3 coats of clear nail varnish (which is common practice in microleakage studies) [8]. This also ensured that the indicator used in the solution to enable identification of microleakage (methylene blue dye) did not contaminate the cement via the wood.

A jig was designed and built which enabled multiple testing to be carried out, in a liquid, using an Instron 8511 load testing machine. A sample number of 10 was chosen in order to ensure that an accurate picture of the effects of loading were obtained. Constant temperature (of 37 °C) was achieved using a heater and thermistor located in the tank. In order to carry out a torsional test in a compression/tension machine, the specimens were oriented in the horizontal plane with a load applied on a lever arm in order to apply both torsional and bending forces. The forces were applied to the specimens via a series of plunger feet (Fig. 3) contained within a block,

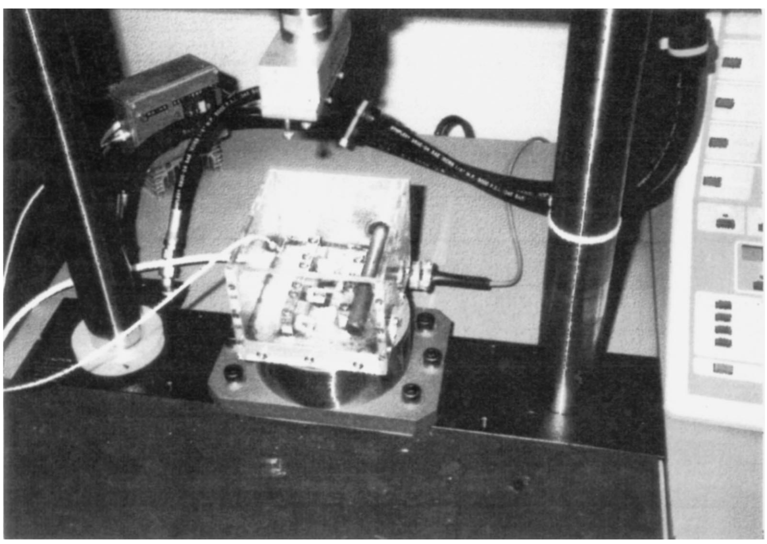

Figure 3 Test jig located on Instron 8511 load testing machine.

and positioned in such a way that their height could be varied to ensure that all specimens were loaded from the same zero position.

The applied cyclic load was determined following testing to failure of the test piece when subjected to a static torsional and bending loading. The magnitude of applied load was 70% of the load to failure.

A test sequence running at 6 Hz for 60,000 cycles between limits of 0 and 250 N of compressive force was developed. 60,000 cycles were chosen in order to represent approximately one year of chewing [13]. Displacement control was used to define the limits of movement of the crosshead in addition to a facility called Advanced Amplitude which also allowed limits of load to be specified. This ensured that control of the limits within the range were achieved and retained for the duration of the test. The maximum and minimum positions and loads achieved throughout the tests were recorded at a sample rate of every tenth cycle. Following completion of 60,000 cycles, the specimens were left in the 37 °C 10% buffered to pH 7.0 methylene blue solution for 24 hours prior to inspection.

A control group for each of the cement types consisted of 2 test pieces. Once prepared, the test pieces were maintained in a water bath at 37 °C for 24 hours to allow the cement to set (as in the test groups). The test pieces were then transferred to a methylene blue solution, again at 37 °C, for 48 hours prior to sectioning and inspection.

2.1. Post preparation and inspection of test pieces

The specimens from the test groups and control groups were reduced in size as shown in Fig. 4, using a Beuhler diamond saw and set in a cold curing phenolic resin in the orientation shown. This was to enable grinding and polishing of the samples to be carried out using a Beuhler multi-polishing machine. The amount of material removed as a result of the grinding and polishing operations was approximately 0.75 mm. Five sections of each test piece were inspected in order to gain an understanding of the progression of cracking and microleakage throughout the specimen. All specimens were continually stored in water during the inspection procedures, in order to prevent the cement from drying out and cracking as a result of lack of moisture.

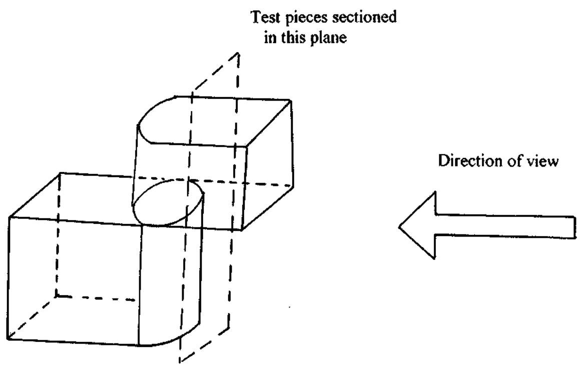

Figure 4 Preparation of test piece for inspection.

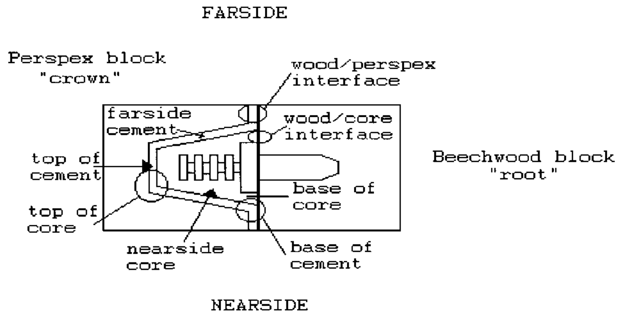

Figure 5 Terminology used in inspection of test piece.

A stereo microscope in conjunction with Beuhler Image Analyser software was used to examine the sectioned test pieces. This enabled identification of cracking in the cement layer and core and also identification of microleakage (dye penetration) into the cement layer and core as a result of ingress at the boundaries. Surface inspection was carried out at a magnification of 50x and images of cracking or other typical features were recorded.

3. Results

The test pieces were prepared and inspected as described above.

The existence of cracking and microleakage in the cement and core test pieces for the three types of cement was recorded with respect to the location of the feature (Fig. 5) and also the rate of occurrence of the feature (Table I) within the test group. The results presented illustrate typically recorded features of cracking and microleakage in the cement layer and core of the test pieces. For the purpose of the analysis of results, the cement layer and core were divided into 8 areas, with additional information given on cracking in the core.

3.1. Cement Layer

3.1.1. Cracking

It can be seen (Table I) that, in general, cracking of the cement layer, when considering all areas which were inspected, occurred with greatest frequency in the zinc phosphate cement and least often in the composite resin cement, in which there were no instances of cracking either at the wood/perspex interface or at the top of the test piece. Cracking at the base of the cement layer in $ZnPO_4$ and RMGI occurred in 80% and 90% of test pieces respectively. This frequency was reduced to 45% in CRC test pieces. In RMGI and CRC, cracking at the base was most commonly a result of a change in profile of either the perspex or the core, or as a consequence of a void in the cement layer at the wood/perspex interface (Fig. 7). In $ZnPO_4$ cement, a change in profile of the core can be seen to induce cracking, however cracking is seen to be initiated from the corners of the perspex piece and also in the area around the base of the cement layer from no apparent source. Analysis of the magnitude of stress/strain as a result of the applied torsion identified the highest strains being recorded at the base of the cement. Therefore, increased cracking in this area would be expected.

TABLE I Summary of results for three cement types

	Cement layer				Core		
	Zinc phosphate	Resin modified glass ionomer	Composite resin cement		Zinc phosphate	Resin modified glass ionomer	Composite resin cement
Cracking				*Cracking*			
Base: Nearside	6	8	5	Base: Nearside	2	4	4
Base/Farside	10	10	4	Base/Farside	1	4	1
Nearside	10	5	5	Nearside	3	6	3
Farside	10	4	6	Farside	7	5	3
Top: Nearside	2	3		Top: Nearside	1	4	1
Top/Farside	4	4		Top/Farside	2	4	
				At Flange of post	8	8	6
Interface: Nearside	2	1		wood/core interface		2	1
(wood/perspex) Farside	2	1					
				across core	4	5	1
				across core and cement	5	3	
Microleakage				*Microleakage*			
Base: Nearside	2	7	8	Base: Nearside	1	2	
Base/Farside		7	6	Base/Farside		3	2
Nearside		4	5	Nearside	1	1	
Farside	1	5	3	Farside	1		
Top: Nearside		2	1	Top: Nearside		1	
Top/Farside		1		Top/Farside		1	
Interface: Nearside		1	3	At post		4	
(wood/perspex) Farside		1	2				

Cracking along the length of the test-pieces occurred in all of the $ZnPO_4$ test group and in approximately 50% of the other two groups. Cracking of the zinc phosphate cement typically occurred across the cement from perspex to the core (Fig. 9). There were also cases of cracking along the length of the cement and along the boundary between cement and core, although less frequent. In the RMGI and CRC test groups, cracking was observed across the cement layer as seen in $ZnPO_4$, but the frequency of these cracks was much reduced in these two groups. Cracking of the cement layer in RMGI test-pieces was more commonly in a random pattern (Fig. 8) or along the boundary between the cement and core, or cement and perspex. In the CRC test group, although cracking of the cement layer occurred, it was often difficult to identify due to the small scale of the cracks. Cracking was observed both across the cement layer (Figs 6 and 9) and also along the boundaries of the system (Fig. 8).

Cracking in the cement layer at the top of the core was identified in the $ZnPO_4$ and RMGI cements, with no cracking in this area of the CRC test pieces. The frequency of cracking at the top of the test pieces was approximately 30–35%. Cracking at the top of the cement layer was seen to extend from the corner of either the perspex or core through the cement layer.

At the wood/perspex interface, there were few recorded instances of cracking, although cracking was recorded in 20% of the $ZnPO_4$ test pieces and 10% of the RMGI test pieces. In some of the test pieces, there was no cement layer at some points of the wood/perspex interface. This may have been a result of the core protruding at locations around the base of the core, thus not permitting cement to be forced back out of the crown into this area. In some instances the core was offset, which then formed a thicker cement layer on one side of the test piece than the other.

3.1.2. *Microleakage*

The $ZnPO_4$ test group demonstrated minimal traces of microleakage in the cement layer. There were two recorded instances of dye at the base of the cement layer (Fig. 11) and one along the length of the cement layer at the perspex/cement interface.

Both the RMGI and CRC test pieces exhibited extensive occurrence of leakage into the cement layer. In both the RMGI and CRC test groups, 70% of test pieces experienced microleakage at the base of the cement layer. In the RMGI group, leakage can be seen as dark areas at the base of the system, usually extending up into the cement layer from the perspex/wood interface. There were also small isolated pockets of dye observed along the cement layer (Fig. 10) and dye identified along the cement/core interface. The CRC test pieces displayed similar microleakage patterns at the base of the test pieces, with the source of dye being from the wood/perspex interface. The dye identified in the cement layer along the length of the core extended from the areas identified as having dye in the base of the cement layer.

3.2. Core

3.2.1. *Cracking*

Cracking of the core was observed in all of the test groups. At the base of the core, the highest frequency of cracking was observed in the RMGI test group (40%). The cracking at the base of the RMGI test pieces originates from the flange of the post extending up into the core (Fig. 13). In the CRC and $ZnPO_4$ test groups, the cracking at the base of the core more often originates from cracking in the cement layer. Cracking along the length of the core was observed in half of the test pieces in the $ZnPO_4$ and RMGI groups, and in 30% of the CRC group. Cracking in the core commonly originated from

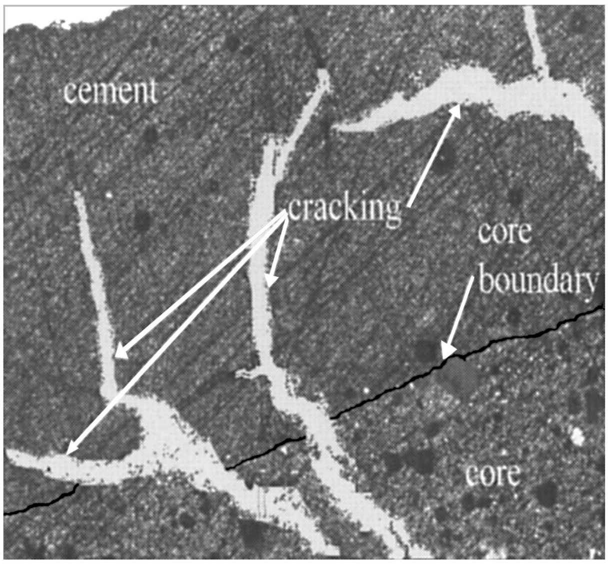

Figure 6 Cracking in the cement layer which seems to have initiated in core.

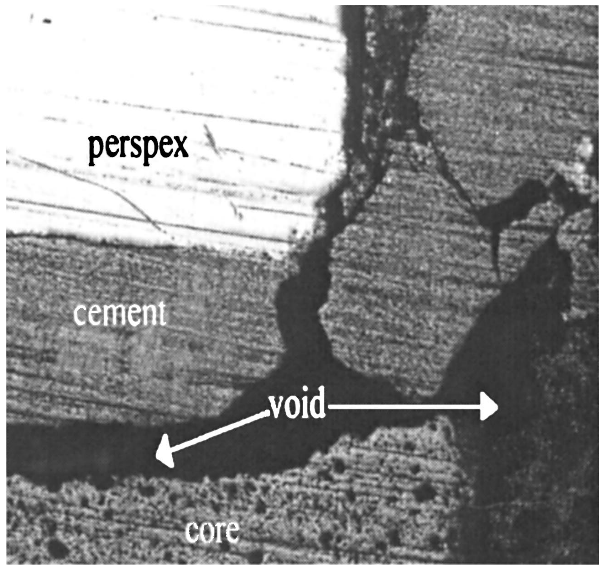

Figure 7 Cracking in two locations at base of cement layer. Void apparent between perspex and cement layer.

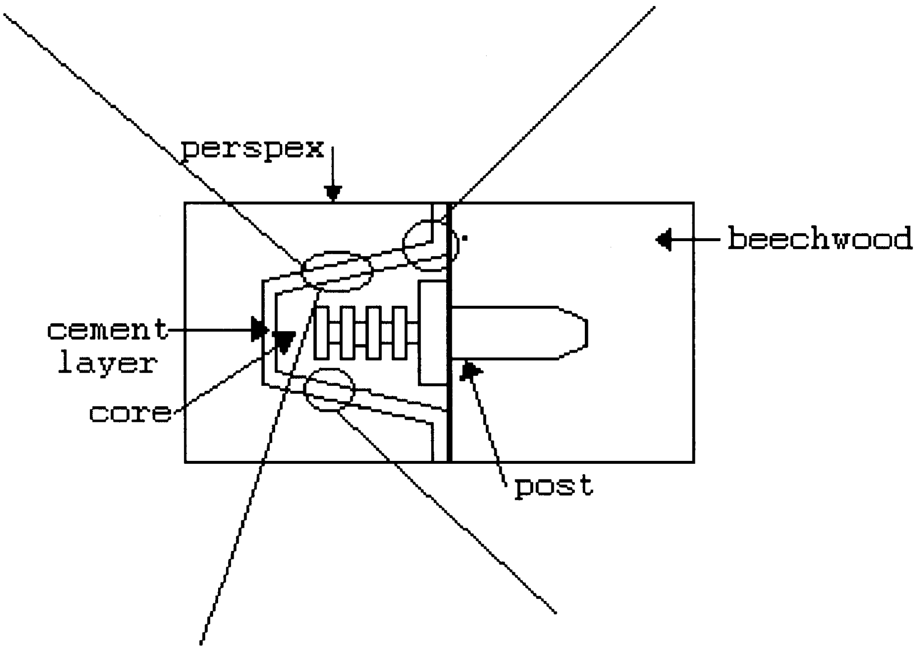

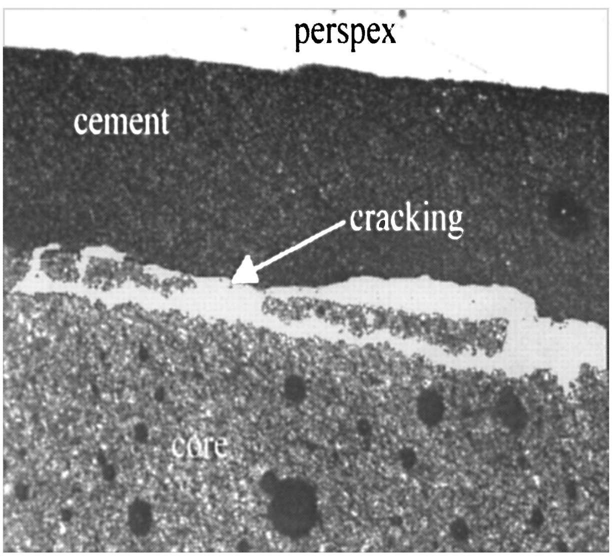

Figure 8 Cracking in core parallel to edge of system.

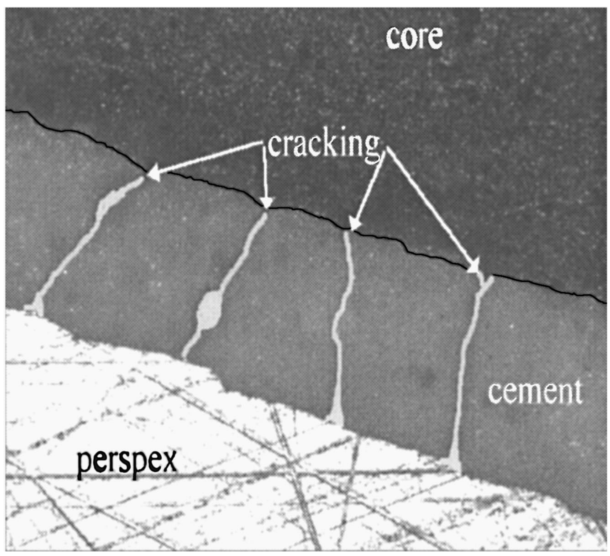

Figure 9 Cracking across the cement layer from perspex to core. Cracks are perpendicular to the length of the core.

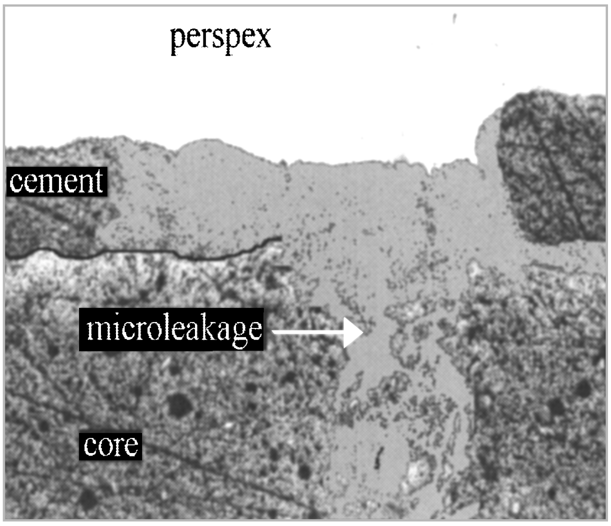

Figure 10 Area of microleakage along side of core from leakage along core/cement interface and into core.

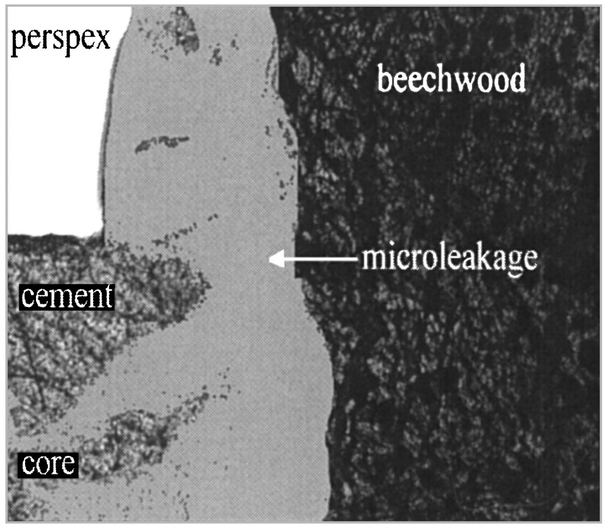

Figure 11 Microleakage from boundary of cement into base of both cement layer and core and progressing along the length of the cement at cement core interface.

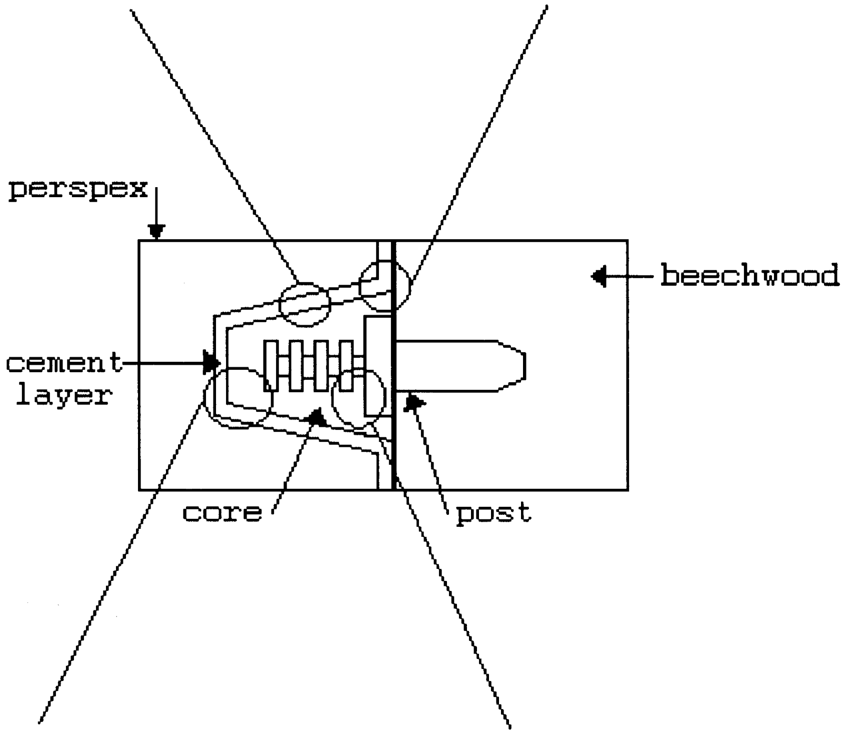

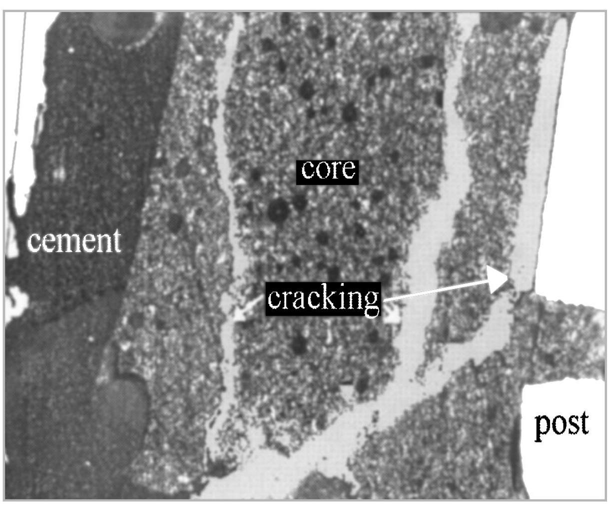

Figure 12 Extensive cracking towards top of core from post and uneven core profile.

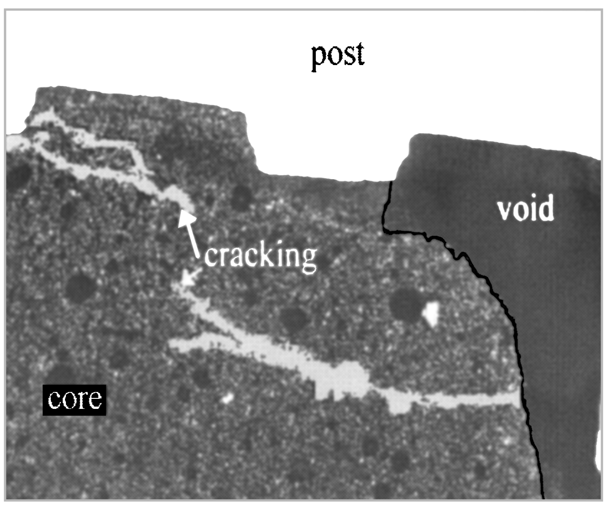

Figure 13 Void in core at flange of post with crack from void into core and crack initiating from serrated edge of post.

TABLE II Summary of results from control groups

	Cement layer				Core		
	Zinc phosphate	Resin modified glass ionomer	Composite resin cement		Zinc phosphate	Resin modified glass ionomer	Composite resin cement
Cracking				*Cracking*			
Base: Nearside	2	1	1	Base: Nearside		1	1
Base/Farside	2	1	1	Base/Farside			
Nearside	2	1		Nearside		1	
Farside	1		2	Farside			
Top: Nearside				Top: Nearside			
Top/Farside				Top/Farside			
				At Flange of post			
Interface: Nearside				wood/core interface			
(wood/perspex) Farside				across core	2		1
				across core and cement			
Microleakage				*Microleakage*			
Base: Nearside		2	1	Base: Nearside			
Base/Farside		1	2	Base/Farside			
Nearside		1		Nearside			
Farside		1	1	Farside			
Top: Nearside				Top: Nearside			
Top/Farside				Top/Farside			
Interface: Nearside		1	1	At post			
(wood/perspex) Farside							

the post and the serrations along the length of the post. The corners of serrations were found to be the initiation points of a high percentage of the cracks observed. The cracking was seen to extend either across the core from the cement/core interface to the post, or along the length of the post from one step to another. Cracking in the RMGI group was also observed running parallel to the core boundary (Fig. 8). Cracking at the top of the core occurred in 5% of CRC, 15% of $ZnPO_4$ and 40% of RMGI test pieces. The cracks in this area appear to originate from the corners of the post and extend towards the corners of the core. In all 3 groups, a similar cracking pattern was observed (Fig. 12).

Cracking which was observed across the core was either restricted to the core material or continued and extended across the cement layer as well. The CRC group contained only one test piece in which cracking extended across the core. In the $ZnPO_4$ and RMGI groups approximately 50% of the test pieces experienced cracking across the core, with a similar percentage recorded with the crack extending into the cement layer. Again, the initiation of the crack in most cases appears to be the post itself. It can be deduced from this that the CRC is more resistant to shear forces than either the RMGI or $ZnPO_4$ cements.

3.2.2. Microleakage
The highest occurrence of microleakage in the core was in the resin modified glass ionomer test group. Microleakage into the core in the CRC and $ZnPO_4$ groups was minimal, with the recorded leakage less than 10%. In the RMGI group, there was evidence of dye at the base of the core in 50% of test pieces, and 40% of test pieces were observed as having microleakage extending into the base of the core. The microleakage most commonly continued along the core/wood interface and into the base of the core surrounding the flange of the post (Fig. 11). The incidence of dye located along the length of the core and at the top of the core was less than 10%.

3.3. Control groups–cement layer
3.3.1. Cracking
Table II contains a summary of results from the control groups of the 3 cements. It can be seen from the data that all groups were recorded as having cracked at the base of the test-pieces and also in the cement layer along the length of the core. The $ZnPO_4$ cement had the highest incidence of cracking in these two locations, with the frequency of occurrence of cracks in the RMGI and CRC groups being similar. No cracking was observed in any other location around the cement layer.

3.3.2. Microleakage
Microleakage was identified in the cement layers of the RMGI and CRC test pieces at the interface, base and along the length of the core. No leakage of dye was recorded at the top of the test pieces. The $ZnPO_4$ test pieces were discovered to have no leakage of dye into the cement in any location.

3.4. Control groups–core
3.4.1. Cracking
Limited cracking of the core of the test pieces was seen in the control groups of all cements. However the frequency of these was low, and there does not appear to be a pattern to the cracking that existed.

3.4.2. Microleakage
No microleakage was seen in the cores in any of the test pieces in the control groups.

4. Conclusions

A method has been developed using cyclic load testing and image analysis to investigate the effect of varying one component in a post/crown system. The results from these investigations confirmed that this technique is capable of identifying a variation in the behavior of the cement under investigation and also the effect of this component on the materials which it comes into contact with. From these investigations it was also shown that microleakage assessment techniques provide valuable information on the state of a system following mechanical load testing. As a result of this it was shown that this technique is valuable in the analysis of new luting cements for use in dentistry. Further investigations could possibly establish whether or not the effect of varying the core material in the system, or the type of endodontic post used, can be detected using this technique.

References

1. STANDLEE, J. P., CAPUTO, A. A., HOLCOMB, J. and TRABERT, K. C., *Journal of Prosthetic Dentistry*, **44**(4) (1980) 398–404.
2. RICKER, J. B., LAUTENSCHLAGER, E. P. and GREENER, E. H., *Dental Materials*, **2** (1986) 63–66.
3. JOHNSON, J. K. and SAKUMURA, J. S., *The Journal of Prosthetic Dentistry*, **40**(6) (1978) 645–649.
4. CHAPMAN, K. W., WORLEY, J. L. and FRAUNHOFER, J. A., *General Dentistry*, **33** (1985) 128–130.
5. STANDLEE, J. P. and CAPUTO, A. A., 1992 *Journal of Prosthetic Dentistry*, **68**(6) (1992) 913–917.
6. MITCHELL, C. A., Queens University of Belfast, Ph.D. Thesis (1995)
7. WILSON, N. H. F., SETCOS, J. C., DUMMER, P. M. H., GORMAN, D. G., HOPWOOD, W. A., SAUNDERS, W. P., HUGHLOCK, R. J. and HUNTER, M. J., *Quintessence International*, **28**(11) (1997) 737–743.
8. SAUNDERS, W. P., SAUNDERS, E. M. and GUTMANN, J. L., *International Endodontic Journal*, **27** (1994) 325–329.
9. FAN, P., NICHOLLS, J. I. and KOIS, J. C., *International Journal of Prosthodontics*, **8**(3) (1995) 213–220.
10. LIBMAN, W. J. and NICHOLLS, J. I., *The International Journal of Prosthodontics*, **8**(2) (1995) 155–161.
11. INGDONG, O. H., *Hip Society Award Papers*, **8** (1983).
12. LEAHY, J., M.Sc. Thesis, Biomedical Physics and Bioengineering Department, University of Aberdeen (1994).
13. D'ARCY, S., Ph.D. Thesis, School of Mechanical and Offshore Engineering, The Robert Gordon University, Aberdeen (1997).

Received 19 March and accepted 15 July 1998